Quantum Tunneling of Magnetization under Pressure in the High-Spin Mn_{12} Molecular System

Georgiy G. Levchenko,*,† Eduard E. Zubov,† Viktor N. Varyukhin,† Ana B. Gaspar,‡ and Jose A. Real‡

A.A. Galkin Donetsk Physical-Technical Institut NAS of Ukraine, R.Luxemburg, 72, 83114, Donetsk, Ukraine, and Institut de Ciencia Molecular/Departament de Química Inorgánica, Universitat de València, Doctor Moliner 50, 46100 Burjassot, Spain

Received: April 8, 2004; In Final Form: August 12, 2004

Experimental and theoretical investigations of quantum tunneling magnetization in the high-spin cluster $[Mn_{12}O_{12}(CH_3COO)_{16}(H_2O)_4]\cdot 2CH_3COOH\cdot 4H_2O$ under pressure have been performed. The main observation is that the blocking temperature and hysteresis width decrease under the effect of pressure. However, the position of the steps in the magnetization versus field curve does not change noticeably as pressure increases. A theoretical examination of the pressure influence on the relaxation rate and magnetization has been carried out taking into consideration the quantum tunneling effects. The qualitative agreement between theory and experiment has been achieved both at atmospheric and at high pressures. The main conclusion of this analysis is that pressure decreases the blocking temperature, the hysteresis width, and the single ion anisotropy and modifies quantum tunneling magnetization.

Introduction

Quantum tunneling magnetization (QTM) has been subject of much interest since it was considered theoretically.[1−8] The determination of the limit at which the quantum mechanical behavior at the microscopic level underlies the classical behavior at the macroscopic level has been the driving force of this research. In this regard, much attention has been paid to the high-spin molecule $[Mn_{12}O_{12}(CH_3COO)_{16}(H_2O)_4]\cdot 2CH_3COOH\cdot 4H_2O$, herein referred to as Mn_{12}.[9−18] The magnetic behavior of this molecule bridges the atomic and nanoscopic scales because the molecular dimensions determined by the longest metal-to-metal distance (8.6 Å) are around 17 Å

The molecule is made up of 12 manganese ions. Four of them (Mn^{4+}, $S = {}^3/_2$) are disposed in a central tetrahedron surrounded by 8 Mn^{3+} ($S = 2$) ions. Exchange interactions inside the Mn_{12} cluster stabilize a ferrimagnetic-like ground state with a resultant spin value of $S = 10$. Because of the strong magnetic anisotropy, Mn_{12} clusters display superparamagnetic behavior with a blocking temperature of 3.2 K.[9,12,15,16] For temperatures lower than 3.2 K, magnetization versus magnetic field (M vs H) plots display large hysteresis loops characterized by a succession of steep and flat regions when the field direction is opposite of the magnetization.[9,15,16] The distance between these steps is around $\Delta H = D/g\mu_B \approx 0.44$ T, where D is a parameter that represents single ion anisotropy (SA) for the molecule. These steps are stipulated by temperature assisted quantum tunneling between S_m and S_{-m+1} states through the single ion anisotropy barrier.

Although the physical picture of Mn_{12} magnetization in magnetic field is qualitatively clear, the study of the crossover of quantum mechanical and classical behaviors is not yet a fully characterized problem. The effect of pressure on these phenomena could be a useful tool for getting additional information. The influence of pressure on QTM has previously been studied.[18,19] Significant suppression of QTM by pressure and an increase in the first step in the M versus H curve are the main findings of these studies, which have opened new ways to tune QTM. In this context, we consider that the study of the quantum tunneling phenomenon under pressure is still a current open question. Consequently, we have investigated the effect of hydrostatic pressure on the QTM as well as on the relaxation processes of Mn_{12}. We have determined the effects of pressure on SA from independent measurements of the blocking temperature and hysteresis loops. We also have used the determined D values to calculate the temperature and field dependences of magnetization in the frame of a quantum mechanical approach. Finally, we also compare these calculations with our experimental data.

Experimental Section

Sample Preparation. The sample constituted of single crystal needles (10 μm in size), has been synthesized according to the method published elsewhere, and its identity was checked using single-crystal X-ray analysis.[20]

Magnetic Measurements. The variable temperature magnetization measurements were carried out on samples constituted by small single crystals (∼10 μm) using a Quantum Design MPMS2 SQUID magnetometer. The magnetic measurements under pressure were performed using a hydrostatic pressure cell, specially designed for our SQUID set up and made up of hardened beryllium bronze with silicon oil as the pressure transmitting medium operating in the pressure range of 1 bar−12 kbar. The pressure was measured by taking advantage of the pressure dependence of the superconducting transition temperature of the built-in pressure sensor constituted of high purity tin.

The small single crystals were packed in a cylindrically shaped aluminum sample holder of 1 mm in diameter and 6−7

* Corresponding author: E-mail: levch@levch.fti.ac.donetsk.ua.
† A.A. Galkin Donetsk Physical-Technical Institut NAS of Ukraine.
‡ Universitat de València.

10.1021/jp048446f CCC: $27.50
Published on Web 10/02/2004

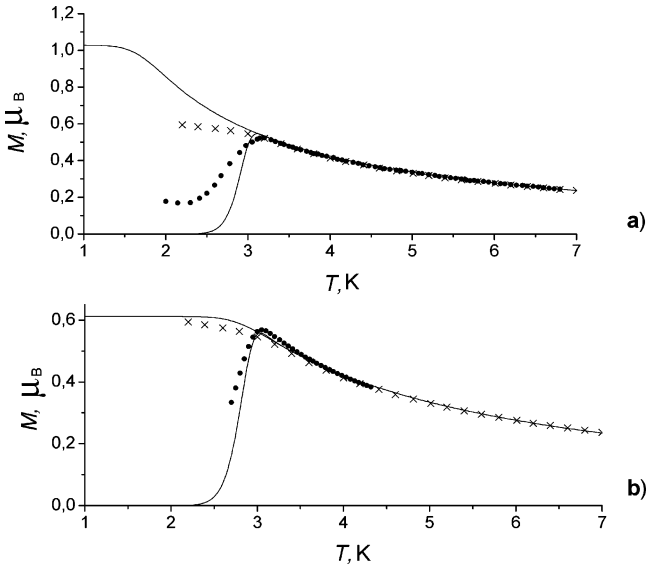

Figure 1. Field cooling (×), and zero-field cooling (●) experiments for Mn_{12} cluster. Theoretical behavior is represented by solid lines for: (a) $P = 1$ bar, $\tau_0 = 10^{-8}$ s, $T_B = 3.2$ K, and $D = 0.69$ K and (b) $P = 10$ kbar, $\tau_0 = 2 \times 10^{-7}$ s, $T_B = 3.05$ K, and $D = 0.586$ K.

mm in length. To align the easy axis of the crystallites along the direction of the magnetic field, we carried out the following procedure. In the first stage, the sample placed in the oil medium, in the high-pressure cell, was cooled from room temperature down to 20 K at 5 T. At this temperature, the orientation of the crystals is fixed by frozen oil. Then, zero field cooling (ZFC) or field cooling (FC) measurements were performed at 10^{-2} T with an average measuring time of 22 s. The accuracy was ±0.01 K for temperature and ±0.25 kbar for pressure. The magnetization curves were measured at 2 K, and the magnetic field was increased stepwise with an average rate of around 1.6×10^{-4} T/s. The magnetic field was increased by steps of 10^{-2} T, and the magnetic moment was relaxed over one minute to its equilibrium value for each applied magnetic field.

Results

Figure 1a and b displays the ZFC and FC curves at $P = 1$ bar and at $P = 10$ kbar, respectively. The FC magnetization curve increases as temperature decreases in the whole range of temperatures measured, whereas the ZFC magnetization increases at the beginning and then decreases as temperature increases. The characteristic temperature of the M versus T curve at the maximum corresponds to the blocking temperature, T_B, and is equal to 3.2 K at $P = 1$ bar. This maximum is shifted by pressure to low temperatures, reaching a value of $T_B = 3.05$ K at $P = 10$ kbar.

The magnetic field dependences of magnetization, displayed in Figure 2a and b, were measured at 2 K and 1 bar and 9.5 kbar, respectively. Essentially, a shift of the M versus H curve to low fields is observed when the pressure is changed from 1 bar to 9.5 kbar. This fact is a consequence of the slope increase that was observed in the zero field at 9.5 kbar. In contrast, the steps of M versus H curve were not shifted noticeably by pressure. The maximums of the $^{dM}/_{dH}$ versus H curves (Figure 3) display a small shift to high field as previously reported.[18] This shift is caused by the displacement of the position of the first step. The distances between the other maximums are the same as those at atmospheric pressure in the limit of experimental accuracy. The step observed at around 1.75 T, at 1bar, almost disappears at 9.5 kbar.

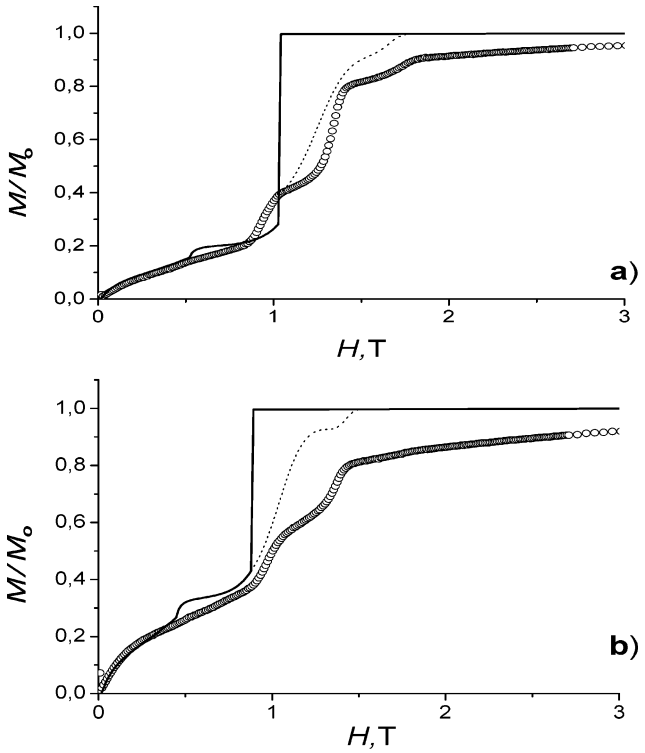

Figure 2. Experimental and calculated magnetization (M/Mo) of Mn_{12} as a function of magnetic field at $T = 2$ K: (a) $P = 1$ bar. (○) experiment; (−) theory at $D = 0.69$; (−) at μ_B g Hx/$k_B = 0.032$K, (- - -) at μ_B g Hx/$k_B = 0.001$ K. b) P = 9.5 kbar. (○) experiment; (−) theory at $D = 0.586$; solid line at μ_B g Hx/$k_B = 0.032$K, dotted line at μ_B g Hx/$k_B = 0.001$K, Mo−saturating magnetization.

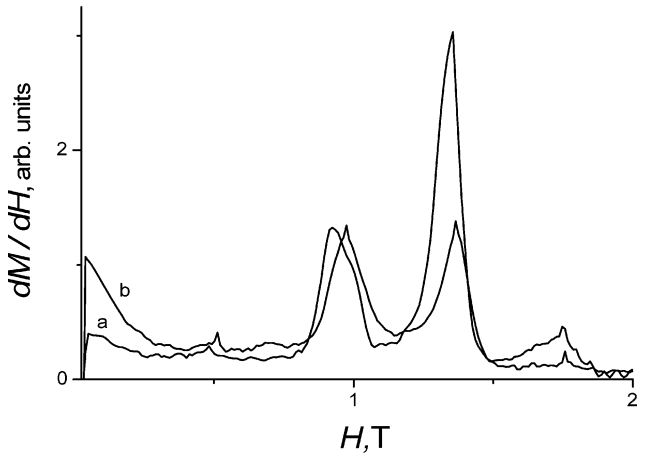

Figure 3. Field dependence of the derivatives $^{dM}/_{dH}$ for Mn_{12} at 2 K under pressures: (a) P = 1 bar and (b) at P = 9.5 kbar.

Figure 4 displays M versus H hysteresis loops for 1 bar, 5.8 kbar, and 8.2 kbar experiments at 2 K. A decrease in the hysteresis width takes place concomitantly to an increase in M, at low fields, as pressure is increased.

Analysis and Discussion

The essential physics of single-molecule magnets originates from its large total spin S and an axial magneto-crystalline anisotropy (DS_z^2, with $D < 0$). To a fairly good approximation one can describe such a giant spin by the following effective spin Hamiltonian[21,22]

$$\mathrm{H} = DS_z^2 + \mu_B g H_z S + E(S_x^2 - S_y^2) + O_4 + H' \qquad (1)$$

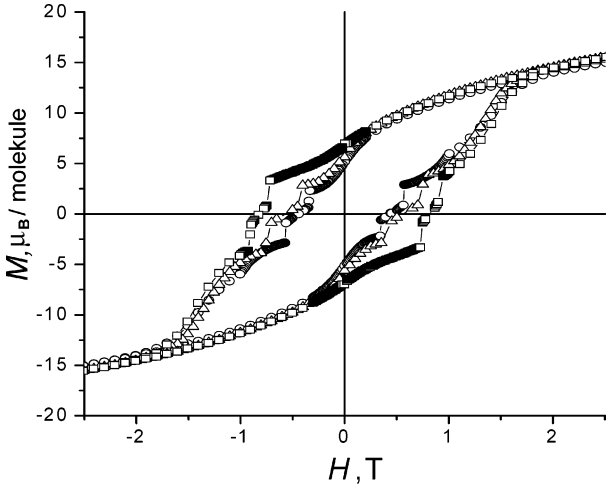

Figure 4. Magnetization loops of Mn_{12} as a function of applied magnetic field at $T = 2$ K under pressures $P = 1$ bar (□), $P = 5.8$ kbar (△), and $P = 8.2$ kbar (○).

where the first term is the magneto-crystalline anisotropy energy, the second term is the energy of the cluster in the external magnetic field aligned along the easy axes, the third and fourth terms are the second- and fourth-order transverse anisotropies energies, respectively. H' denotes the environmental couplings such as hyperfine, dipolar, and exchange interactions.

Recently, on the basis of a detailed X-ray diffraction analysis, it has been shown that six different isomeric forms of the Mn_{12} cluster can be envisaged.[23] As a result, it has been concluded that the average molecular symmetry of these clusters is lower than axial and that the transfer anisotropy plays an essential role, especially for the description of ESR experiments and transitions between more than two degenerated levels.[22,23] However, one can qualitatively describe the magnetic field dependence of magnetization with the following spin Hamiltonian[3,24!]

$$\mathrm{H} = -DS_z^2 - \mu_B g(H_z S_z + H_x S_x) \tag{2}$$

where H_x is the perturbing magnetic field along the x direction. H_x consists of the transfer field of any origin mentioned above. H_x also includes the transfer field caused by the misalignment of the applied field with respect the easy axes. D is the average anisotropy barrier. Here, it is supposed that $H_x \ll H_z$. When H_x is neglected, the solution of this Hamiltonian shows that in the applied field $H_z = H_k = k\mathrm{D}$ ($k = 1-N$), the spin levels ϵ_m and $\epsilon_{m'}$ in the two wells have the same energy at $m' = -m - k$ for $m < 0$. The transition experienced by the spins between opposite applied field directions and those aligned to the applied field directions is driven by thermal excitation, assisted by one- or two-phonon absorption or emission.

The existence of a potential barrier between two stable states of magnetic moments leads to the appearance of a strong relaxation effect in temperature and field variation of magnetization. In the classical case, the relaxation time for superparamagnetic particles follows the Arrhenius law[25]

$$\tau = \tau_0 \mathrm{e}^{U/k_B T} \tag{3}$$

where U represents the energy of the potential barrier, which is equal to DS^2 in the case of SA, τ_0^{-1} is the rotational frequency of the magnetic moment in the magnetic field, which is suggested to be around 5×10^8 s^{-1}.[26] On the basis of eq 2, it

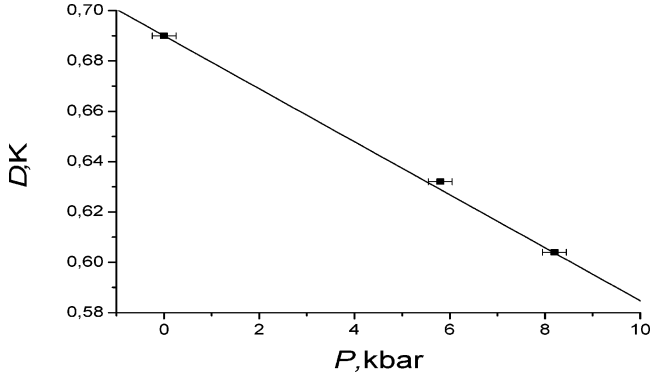

Figure 5. Pressure dependence of single ion anisotropy (D).

is easy to determine T_B for the magnetic moment down from which the measuring time becomes comparable with τ

$$T_B = \frac{DS^2}{k_B \ln\left(\frac{t}{\tau_0}\right)} \tag{4}$$

If we take the experimental values $T_B = 3.2$ K, $D/k_B = 0.69$ K, and measuring time $t = 22$ s, then we get $\tau_0 = 10^{-8}$ s, in agreement with the results previously reported,[26] which confirms the acceptable value of the measuring time.

For temperatures below T_B, the coercive force is determined as follows[27]

$$H_{coerc}(T) = H_{coerc}(0)\left(1 - \sqrt{\frac{T}{T_B}}\right)K \tag{5}$$

where $H_{coerc}(0) = 2U/M = 2DS/\mu_B g = 2H_A$ is the coercive force at $T = 0$ K, $M = \mu_B g S$ is the magnetic moment per molecule, and H_A is the anisotropy field. The coefficient K in eq 5 is determined by taking into consideration that a chaotic distribution of molecular magnetic moments of different orientations exists even in the presence of a strong magnetic field. It is possible to show the point when the polar axes of the magnetic moments are randomly oriented, which is the case of $K = 0.5$.

From eq 4 at $t = \tau = 22$ s,

$$H_{coerc}(0) = \frac{43 k_B T_B}{M} \tag{6}$$

Using the experimental blocking temperature $T_B = 3.2$ K, a value of $H_{sat} = H_{coerc}(0) \approx 102$ kOe is obtained from eq 6. In addition, an anisotropy field H_A equal to 51 kOe, which is half of $H_{coerc}(0)$, can be inferred from the experimental value of $D = 0.69$ K. These values agree quite well.

Using the experimental value of the coercive field determined from the hysteresis loops (see Figure 4) at different pressures ($P = 1$ bar, 5.8 kbar, and 8.2 kbar) and assuming that K is independent of pressure, the dependence of the SA parameter on pressure was obtained. To do so, we first evaluated the dependence of T_B on P from eqs 5 and 6 and, finally, the plot of D versus P was derived from those equations. Figure 5 displays the linear dependence of the D versus P plot. The parameter D is not a pure single ion anisotropy parameter because it was obtained from the magnetic field dependence of magnetization measurements. It represents the total anisotropy barrier and includes the average anisotropy of all isomers and some part of the transfer anisotropy.

For an aid to understanding the mechanism of pressure dependence of the M versus H curves and the relaxation rate Γ,

we included, in a further consideration, the variation of D with pressure. To do so, we considered the following differential equation for a number of particles in two potential wells for the case of the high potential barrier[28]

$$\frac{dn_1}{dt} = -\frac{dn_2}{dt} = n_2\nu_{21} - n_1\nu_{12} \tag{7}$$

where ν_{12} and ν_{21} represent the probability of transitions of the particles per unit of time from well 1 to well 2 and from well 2 to well 1, respectively. These probabilities were evaluated in the frame of a classical thermodynamic potential[28] with the total number of particles, $n = n_1 + n_2$, being independent of time. In the frame of a quantum mechanical consideration, eq 7 has the same form if one neglects tunneling effects. In this case, eq 7 has a simple relaxation type of solution, and the expression for the relaxation rate $\Gamma = \nu_{12} + \nu_{21} = {}^1/_\tau$ was determined to be[24]

$$\Gamma = \frac{1}{N_s N_{-s}} \left[\sum_{m=-S}^{S-1} \frac{1}{(S(S+1) - m(m+1))(2m+1)^2 \gamma_a(\omega_{m+1,m}) N_m}\right]^{-1} \tag{8}$$

where $N_m = \exp(-\epsilon_m/k_B T)/\Sigma_{m=-S}^{S} \exp(-\epsilon_m/k_B T)$ is the population of level m, $\gamma_a(\omega_{mn})$ is the probability of transition from the m level to the n level. The proportionality coefficient for $\gamma_a(\omega_{mn})$ has been determined by equating Γ to ${}^1/_\tau$ in eq 3 at zero magnetic field.

To take into consideration tunneling effects, one should include the normal weak perturbing component of the effective field, H_x, to the z axis. This induces a mixing of resonant levels m and m', increasing abruptly the probability of a transition between stable and unstable states. To determine the ratio of the amount of spins in the two wells, it is necessary to take the sums of the populations of all quantum levels for every well. In this case, the component determined by the tunneling frequency of the transition of the particle between the two wells is added in eq 7. This frequency is proportional to the square of the splitting of the resonant levels m and $m' = -m - k$ ($\Delta\epsilon_{mm'} \approx (H_x)^{m'-m}$) and is inversely proportional to $\gamma_a(\omega_{mm'})$ at the resonant field $H = H_k$.[24] It is obvious that the ratio $(\Delta\epsilon_{mm'})^2/\gamma_a(\omega_{mm'})$, which determines the probability of transition per unit of time, increases at $\gamma_a(\omega_{mm'}) \rightarrow 0$. Thereby, the quantum mechanical generalization of Neel's theory, with consideration of one-phonon and Raman dissipations on the magnetic moment, allows us to establish the peculiarities of the relaxation rate:[3] (i) the Γ versus H dependence displays an abrupt decrease in the Γ value at intervals of H that correspond to the difference between the corresponding energy levels. It is caused by resonance radiation of phonons at magnetic absorption; (ii) in contrast, quantum tunneling leads to the opposite effect, namely, an abrupt increase in the relaxation rate. In summary, the results of these two effects are the oscillations of the relaxation rate in the magnetic field with maximums at fields $H_k = kD$. Even at $H = 0$, the system has essentially a high relaxation rate, which explains the sharp increase in magnetization at a small magnetic field. This fact contrasts strongly with the classical situation in which the blocking of the magnetic moment takes place for small magnetic field ($H \ll D$) and, consequently, a gentle increase in magnetization is observed.

According to the above-mentioned generalization, the calculated field dependencies of Γ at $P = 1$bar and $P = 9.5$ kbar and at $T = 2$ K are displayed in the Figure 6. These calculations were carried out by taking into account the tunneling current and using the following values: $\mu_B g H_x/k_B = 0.032$ K, $g = 2$, $\tau = 2 \times 10^{-7}$, and $D = 0.69$ K at $P = 1$ bar and $\mu_B g H_x/k_B = 0.032$ K, g = 2, $\tau = 2 \times 10^{-7}$, and $D = 0.586$ K at $P = 9.5$ kbar. $D = 0.586$ is taken from the pressure dependence of D shown in Figure 4. For $H = H_k$, the relaxation rate increases considerably at both pressures. At $P = 9.5$ kbar, the distances between the jumps, of the relaxation rate versus the magnetic field curve, decrease and the jumps become smaller. At both pressures, the magnitude of the jumps decreases as the magnetic field increases.

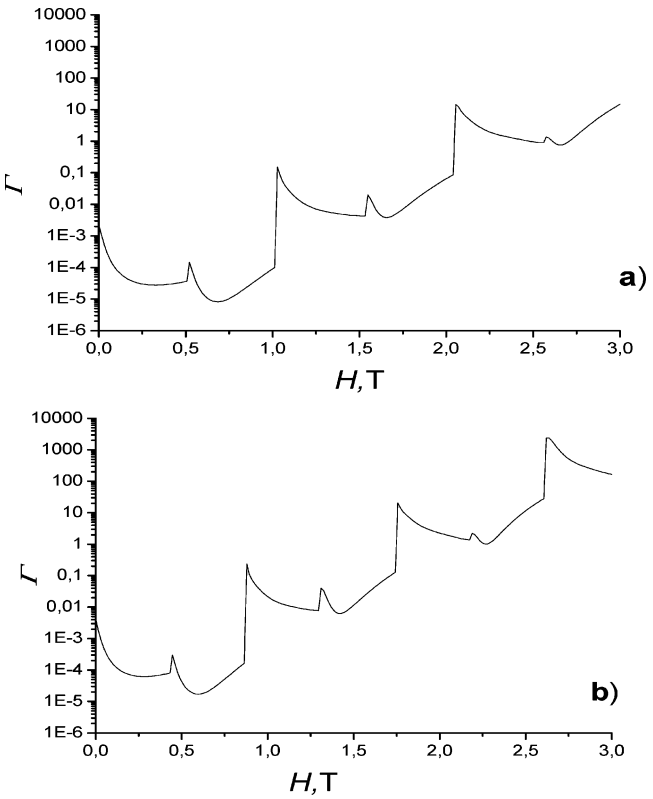

Figure 6. Magnetic field dependence of the relaxation rate (Γ) at $T = 2.0$ K (Raman correction 2%); (a) $P = 1$ bar and (b) $P = 9.5$ kbar.

Additionally, the theoretical magnetization curves, M versus H, at $P = 1$ bar and 9.5 kbar were deduced from the evaluation of eq 7. For that, we used the calculated values Γ. We also considered the fact that, in the experiment, the magnetic field was increased by steps of 10^{-2} T, waiting for intervals of 60 s per step. The whole time of the experiment was divided by these intervals. Consequently, the initial conditions of eq 7 were set up for every interval in agreement with n_i relaxation to its equilibrium value. In this case, at $P = 1$bar, the magnetic field component $\mu_B g H_x/k_B = 0.032$ K and $D = 0.69$ K match quite well the experimental date at small applied fields, showing a strong divergence for applied fields greater than 1 T. Assuming that H_x decreases as the magnetic field increases, for $H > 1$ T, we obtained a good qualitative agreement for $\mu_B g H_x/k_B = 0.001$ K, as it is demonstrated in Figure 2a. For $P = 9.5$ kbar, the best agreement is obtained for the same values of H_x and $D = 0.586$ K. (Figure 2b).

When comparing the calculated and measured M versus H curves, a reasonable agreement is achieved when the deduced pressure dependence of D is used together with the perturbation transfer field H_x. The increase in the first step, induced by pressure in the M versus H curve is also simulated by decreasing

the D value and considering tunneling effects in zero applied field. This increase, first observed in pressure experiments,[19] was explained by static effects stemming, most likely, from transitions between Mn_{12} Jahn−Teller isomers, which may increase the number of fast relaxation molecules. For fast relaxation Jahn−Teller isomers, a D parameter equal to 0.35 K has been deduced.[29] Consequently, these transitions could be one of the reasons for the calculated decrease in D under pressure in the present report.

To understand the reasons of the decrease in H_x with the increase in the external magnetic field, one should take into account the following three points: (i)the isomers with smaller D values are characterized by larger distortions of the octahedral cores[19] and, consequently, a larger H_x, (ii) because of the lack of interactions between the magnetic clusters, they are considered to be isolated units,[21,23] and (iii) in the theoretical calculations, H_x is the same for both pressures. These facts mean that if there are six isomers of magnetic clusters,[23] then the behavior of every isomer with magnetic field increase is individual. It means that, in a first approximation, pressure decreases the D but does not influence the effective value of H_x. It also means that the decrease in D by pressure enhances the quantum tunneling in the zero magnetic field at the same mixing of the levels. Because every isomer behaves independently, tunneling effect at small applied fields takes place in isomers with smaller D values. With the magnetic field increase, the isomers with larger D values and, consequently, with smaller H_x values are magnetized along easy axes. This fact can be the main reason for the observed decrease in H_x as the applied field increases, as well as for the independence of the positions of the $^{dM}/_{dH}$ peaks with the pressure increase. In addition, one can add that because the D is an average anisotropy, the observed position of the peaks is also determined by the distribution of the anisotropy of the isomers. We should not exclude this possibility because the width of the transitions is larger than the calculated shift of the peaks caused by the change in the D under pressure; this is the reason that we determine the D from hysteresis width where we have one point of intersection of magnetization curve and x axis but not from the positions of the peaks.

The temperature dependencies of the equilibrium (FC) and nonequilibrium (ZFC) magnetic moment were calculated in the same way as those at the magnetic field of 10^{-2} T. The previously determined values of H_{sat} and τ under consideration of tunneling effects were used. The results are presented in Figure 1a and b. In these calculations, we have taken also into consideration the fact that the full alignment of the anisotropy axes of all crystallites along the direction of the magnetic field, at high temperatures, was not achieved, and consequently, we have used an adapted ordering coefficient $K = 0.6$ for both pressures. The calculated temperature dependences of magnetization at temperatures higher than T_B coincide with the experimental for both pressures. The calculated values of the blocking temperatures were T_B, = 3.2 K (1bar) and 3.05 K (10 kbar), in agreement with those obtained experimentally. At temperatures lower than T_B, the calculated ZFC curve qualitatively agrees with the experiment, in contrast to the FC curves. Unfortunately, the used approximation does not allow for us to obtain greater agreement for temperatures lower than T_B.

Conclusions

We have reported experimental and theoretical studies on the influence of pressure on quantum tunneling magnetization in Mn_{12} species. Our study confirms the results previously derived.[18,19] Moreover, we have obtained new experimental results and described them in the frame of simple theoretical consideration. The most important findings are (i) the observation of the decrease in the blocking temperature T_B, (ii) the observation of the decrease in the hysteresis loop, (iii) the theoretical analysis of the experimental observations was performed using the determined D value from the measured values of T_B and coercive forces and taking into account quantum tunneling effect, qualitative agreement between theory and experiment is reasonable, and (iv) the observed effect of pressure on the M versus H curves has been described and explained from the combination of the following three factors: decrease of the single ion anisotropy, variation of transfer magnetic field with applied magnetic field, and modification of the relaxation time regime.

The observed slight effect of the pressure on the position of the steps in the M versus H curves is explained by the small pressure dependence of D and by the independent behavior of the magnetization of the different isomers in the applied magnetic field. It is obvious that the increase in the slope at low fields under pressure is also related to the increase of the relaxation rate caused by the decrease of the potential barrier U in agreement with our calculations at $H = 0$.

Acknowledgment. G. L. appreciates financial support from the European Science Foundation (Program Molecular Magnets) and the NATO Scientific Committee. J. A. R. thanks the Ministerio Español de Ciencia yTecnología (projectBQU2001−2928).

References and Notes

(1) Chudnovsky, E. M.; Gunther, L. *Phys. Rev. Lett.* **1988**, *60*, 661.
(2) Hartmann-Boutron, F.; Poloti, P.; Villain, J. *Intern. J. Mod. Phys.* **1996**, *10*, 2577.
(3) (a) Van Hemmen, J. L.; Suto, A.; *Europhys. Lett.* **1986**, *1*, 481. (b). Van Hemmen, J. L.; Suto, A. *Physica* **1986**, *141B*, 37.
(4) Shapira, Y.; Bindillatti, V. *Appl. Phys. Rev.* **2002**, *92*, 4155.
(5) Gard, A.; Kim, G.-H. *Phys Rev. B* **1992**, *45*, 12921.
(6) Loss, D.; DiVincento, D. P.; Grinstein, G. *Phys. Rev. Lett.* **1992**, *69*, 3232.
(7) Chudnovsky, E. M.; Tejada, J. *Macroscopic Quantum Tunneling of the Magnetic Moment*; Cambridge University Press: Cambridge, U.K., 1998; p 185.
(8) Cristou, G.; Gatteschi, D.; Hendricson, D. N.; Sessoli, R. *MRS Bull*. **2000**, *25*, 66.
(9) Barbara, B.; Wernsdorfer, W.; Sampaio, L. C.; Park, J. C.; Paulsen, C.; Novak, M. A.; Ferré, F.; Mailly, D.; Sessoli, R.; Caneschi, A.; Hasselbach, K.; Benoit, A.; Thomas, L. *J. Magn. Magn. Mater*. **1995**, *140−144*, 1825.
(10) Perenboom, J. A. A. J.; Brooks, J. S.; Hill, S.; Hathaway, T.; Dalal, N. S. *Phys. Rev. B* **1998**, *58*, 330.
(11) Paulsen, C.; Park, J.-G. *Quantum Tunnelling of Magnetization*; Gunther, L., Barbara, B., Eds.; Kluwer: Dordrecht, The Netherlands, 1995, pp 189−207.
(12) Tejada, J.; Ziolo, R. F.; Zhang, X. X. *Chem. Mater*. **1996**, *8*, 1784.
(13) Caneschi, A.; Gatteschi, D.; Sessoli, R.; Barra, A. L.; Brunel, L. C.; Guillot, M. *J. Am. Chem. Soc.* **1991**, *113*, 5873.
(14) Sessoli, R.; Tsai, H.-L.; Schake, A. R.; Wang, S.; Vincent, J. B.; Folting, K.; Gatteschi, D.; Christou, G.; Hendrickson, D. N. *J. Am. Chem. Soc.* **1993**, *115*, 1804.
(15) Sessoli, R.; Gatteschi, D.; Caneschi, A.; Novak, M. A. *Nature* **1993**, *365*, 141.
(16) Shwarzschild, B. *Phys. Today* **1997**, 17.
(17) Gomes, A. M.; Novak, M. A.; Sessoli, R.; Ganeschi, A.; Gatteschi, D. *Phys. Rev. B* **1998**, *57*, 5021.
(18) Murata, Y.; Takeda, K.; Sekine, T.; Ogata, M.; Awaga, K. *J. Phys. Soc. Jpn.* **1998**, *67*, 3014.
(19) Suzuki, Y.; Takeda, K.; Awaga, K. *Phys. Rev. B* **2003**, *67*, 132402.
(20) Lis, A. *Acta Crystallogr., Sect. B* **1980**, *36*, 2042.
(21) Barra, A. L.; Gatteschi, D.; Sessoli, R. *Phys. Rev. B* **1997**, *56*, 8192.
(22) Hill, S.; Edwards, R. S.; Jones, S. L.; Dalal, N. S.; North, J. M. *Phys. Rev. Lett.* **2003**, *90*, 217204−1.
(23) Cornia, A.; Sessoli, R.; Sorace, L.; Gatteschi, D.; Barra, A. L.; Daiguebonne, C. *Phys. Rev. Lett.* **2002**, *89*, 257201−1.

(24) Garanin, D. A.; Chudkovsky, E. M. *Phys. Rev. B* **1997**, *56*, 11102.
(25) Neel, L. *Comput. Rend.* **1949**, *228*, 664.
(26) Luis, F.; Bartolome, J.; Fernandez, J. F. *Phys. Rev. B* **1998**, *57*, 505.
(27) Bean, C. P.; Livingston, J. D. *J. Appl. Phys.* **1959**, *30*, 120.
(28) Brown, W. F. *Phys. Rev.* **1963**, *130*, 1677.
(29) Evangelisi, M.; Bartolome, J.; Luis, F. *Solid State Commun.* **1999**, *112*, 687.